Analogs of Reaction Intermediates Identify a Unique Substrate Binding Site in *Candida rugosa* Lipase†

Paweł Grochulski,‡,§ François Bouthillier,‡ Romas J. Kazlauskas,‖ Alessio N. Serreqi,‖ Joseph D. Schrag,‡ Edmund Ziomek,‡ and Miroslaw Cygler*,‡

Biotechnology Research Institute, National Research Council of Canada, Montréal, Quebec H4P 2R2, Canada, and Department of Chemistry, McGill University, Montréal, Quebec H3A 2K6, Canada

Received September 21, 1993; Revised Manuscript Received December 20, 1993®

ABSTRACT: The structures of *Candida rugosa* lipase–inhibitor complexes demonstrate that the scissile fatty acyl chain is bound in a narrow, hydrophobic tunnel which is unique among lipases studied to date. Modeling of triglyceride binding suggests that the bound lipid must adopt a "tuning fork" conformation. The complexes, analogs of tetrahedral intermediates of the acylation and deacylation steps of the reaction pathway, localize the components of the oxyanion hole and define the stereochemistry of ester hydrolysis. Comparison with other lipases suggests that the positioning of the scissile fatty acyl chain and ester bond and the stereochemistry of hydrolysis are the same in all lipases which share the α/β-hydrolase fold.

The commercial potential of organic syntheses catalyzed by lipases (Boland et al., 1991) underscores the need for a comprehensive understanding of lipase structure and function and has provided the impetus for many recent investigations. Consequently, our understanding of lipases has increased dramatically in the past few years. The first three-dimensional structures of lipases confirmed that the active sites are formed by triads similar to those of serine proteases and that conformational changes are associated with the interfacial activation (Brady et al., 1990; Winkler et al., 1990; Schrag et al., 1991). Comparison of the native *Rhizomucor miehei* lipase (RML) with covalent complexes showed that activation involves a rigid body movement of a single helix (Brzozowski et al., 1991; Derewenda et al., 1992). This movement exposes a large hydrophobic surface which is presumed to interact with the lipid interface. The hexyl chain of the bound inhibitor binds in a groove formed by the movement of the helix. The recently reported structure of a noncovalent complex of pancreatic lipase–procolipase–phospholipid, although at lower resolution, shows that activation requires movement of two surface loops, neither of which are rigid body movements (van Tilbeurgh et al., 1993). A large hydrophobic surface is formed by the lipase and by the colipase. Lipid is bound in a depression in the catalytic subunit of the lipase. The association of interfacial activation with rearrangement of the flap was also indirectly supported by the three-dimensional structure of cutinase (Martinez et al., 1992). This enzyme is capable of hydrolyzing triglycerides but does not exhibit the activation by the interface which is typical of lipases. This lack of interfacial activation was attributed to the absence of a flap covering the active site.

Recently, we determined the unliganded structure of a high molecular weight lipase from *Candida rugosa* (CRL) in both open (Grochulski et al., 1993) and closed (Grochulski et al., 1994) conformations. Comparison of these two structures indicates that activation of the lipase requires the movement and refolding, including a *cis* to *trans* isomerization of a proline residue, of a single surface loop to expose a large hydrophobic surface which likely interacts with the lipid interface. We report here high-resolution structures of CRL complexes with the inhibitors *O*-menthyl hexylphosphonochloridate (MPC), hexadecanesulfonyl chloride (HDSC), and dodecanesulfonyl chloride (DDSC), each containing a single alkyl chain.

Kinetic measurements and inhibition studies suggest that the reaction mechanism of lipases involves acylation and deacylation steps similar to those of serine proteases (Chapus et al., 1976; Chapus & Sémériva, 1976) (Figure 1). Acylation of the enzyme results from nucleophilic attack on the ester by the Ser residue of the catalytic triad and proceeds *via* formation of a tetrahedral intermediate (**I** in Figure 1). Deacylation results from nucleophilic attack on the acyl-enzyme by a water molecule, again going through a tetrahedral intermediate (**II** in Figure 1). In both the acylation and deacylation intermediates, an oxyanion is stabilized by hydrogen bonds to protein atoms of the oxyanion hole. The complex of CRL with MPC is an analog of the first tetrahedral intermediate, and the complexes with HDSC and DDSC are analogs of the second tetrahedral intermediate of the reaction pathway. These complexes identify a unique alkyl chain binding tunnel and suggest possible modes of di- and triglyceride binding. These structures, together with those of the unliganded enzyme, provide a solid foundation for understanding the structure–function relationship of this enzyme and will aid in exploiting and controlling its catalytic properties, especially for stereoselective synthesis of fine chemicals.

MATERIALS AND METHODS

The inhibitors 1-hexadecanesulfonyl chloride and 1-dodecanesulfonyl chloride were purchased from Aldrich and Johnson Matthey, respectively, and used without further purification. (1*R*)-menthyl hexylphosphonochloridate was prepared by the tetrazole-catalyzed reaction (Zhao & Landry, 1993) of hexylphosphonic dichloride with (1*R*)-(−)-menthol in the presence of diisopropylethylamine. The reaction selectively replaced one chlorine atom and gave a 1:1 mixture of diastereomeric (S_P,R_P)-(1*R*)-menthyl hexylphosphonochloridate, which was isolated in 18% yield after flash chromatography on silica gel.

† NRCC Publication No. 36159. R.J.K. acknowledges the support of NSERC.

* To whom correspondence should be addressed.

‡ National Research Council of Canada.

§ Permanent address: Institute of Physics, Technical University of Łodź, 93-005 Łodź, Poland.

‖ McGill University.

® Abstract published in *Advance ACS Abstracts*, February 15, 1994.

0006-2960/94/0433-3494$04.50/0

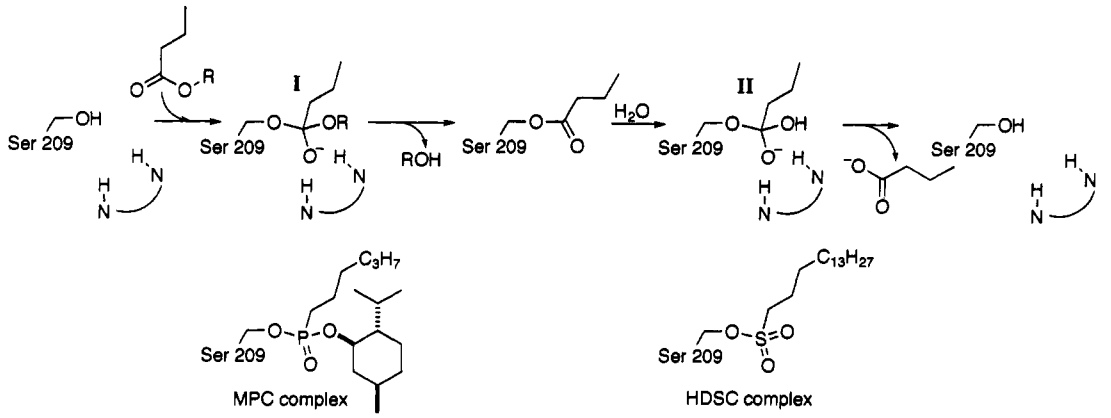

FIGURE 1: Schematic representation of the proposed reaction pathway. The first tetrahedral intermediate, I, arises in the acylation step. The second tetrahedral intermediate, II, occurs during the deacylation step after the attack by a water molecule. The CRL–MPC complex is the analog of I while the CRL–DDSC and CRL–HDSC complexes are analogs of II. The oxyanion hole is shown schematically.

Table 1: Data Collection and Refinement Statistics[a]

	MPC	DDSC	HDSC1	HDSC2	HDSC4	HDSC12	HDSC120
inhibitor:lipase ratio	30:1	10:1	1:1	2:1	4:1	12:1	120:1
resoln range (Å)	8–2.2	8–2.2	8–2.2	8–2.1	8–2.2	8–2.2	8–2.05
space group	$C222_1$	$C222_1$	$C222_1$	$C222_1$	$C222_1$	$C222_1$	$C222_1$
unit cell dimensions							
a (Å)	65.2	65.0	65.0	65.0	65.0	64.9	65.0
b (Å)	97.5	97.4	97.8	97.5	97.6	97.4	97.4
c (Å)	176.3	176.4	176.2	177.1	176.3	176.0	176.2
total no. of observations	68 189	52 448	82 922	82 904	78 113	76 132	83 871
R_{merge} (%)	10.7	7.8	6.8	10.1	4.8	10.6	6.8
completeness of data (%)	84.8	77.4	88.8	87.5	90.1	84.4	86.7
no. of unique reflections	24 584	22 339	25 747	27 893	26 098	24 425	30 119
with $I \geq 2\sigma(I)$	19 378	20 219	23 022	24 234	23 744	19 796	26 705
no. of obsd inhibitor molecules	1	2	1	1	1	2	2
no. of solvent molecules							
H_2O	261	115	160	169	179	178	296
Ca^{2+}	2	2	2	2	2	2	2
no. of sugar molecules	3	3	3	3	3	3	3
final *R* factor							
for $I \geq 2\sigma(I)$	0.136	0.148	0.163	0.157	0.145	0.142	0.136
for all data	0.165	0.160	0.176	0.175	0.155	0.166	0.147
rms deviations from ideality for							
bond lengths (Å)	0.014	0.013	0.014	0.015	0.014	0.013	0.014
bond angles (deg)	2.74	2.74	2.77	2.73	2.66	2.71	2.58
av B-factor (Å^2)	20.0	18.1	19.2	20.9	17.8	18.0	18.0
inhibitor occupancy	1	1/1	0.5	0.7	0.8	1/1	1/1
inhibitor *B*-factor (Å^2)	17	18/34	21	27	24	18/29	19/36

[a] $R_{merge} = \sum_{hkl}\sum_{ref}|I(hkl,j) - \langle I(hkl)\rangle|/\sum_{hkl}\sum_{ref}|I(hkl,j)|$. *R*-factor $= \sum||F_o| - |F_c||/\sum|F_o|$.

Covalent enzyme–inhibitor complexes were prepared by adding the inhibitor dissolved in 2-methyl-2,4-pentanediol (MPD) to the protein solution. Residual lipase activity was monitored by titrimetric assay using triolein as a substrate. The inhibited protein was crystallized under conditions similar to those used for the native protein. At HDSC:lipase ratios of 1:1, 2:1, and 4:1 the enzyme was not completely inhibited before the hanging drops were set up. The His side chains are expected to be doubly protonated since the crystals were grown at pH 5.4. The crystals are isomorphous with the native crystals of CRL in the open form. All diffraction data were collected on a R-AXIS II image plate area detector, and all refinements were done with X-PLOR (Brünger, 1992). Data collection and refinement statistics are shown in Table 1. Refinement of the crystal structures of complexes made with HDSC:lipase ratios of 4:1 and less, assuming full occupancy of the inhibitor, resulted in temperature factors for the inhibitor which were significantly higher than the surrounding protein atoms, suggesting less than full occupancy and consistent with the incomplete inhibition observed before crystallization. The temperature factors were set to values consistent with the surrounding protein atoms, and occupancy was refined. This refinement indicates occupancies of 0.5, 0.7, and 0.8 for HDSC: enzyme ratios of 1:1, 2:1, and 4:1, respectively. Difference maps calculated by excluding the inhibitor molecule show well-defined electron density for the bound inhibitor in all of these crystals. All model building was done using FRODO (Jones, 1978).

RESULTS

Alkyl Chain Binding. The alkyl chains of the inhibitors bind in a long, narrow, hydrophobic tunnel which is unique among the lipases studied to date (Figure 2). The tunnel projects first toward the middle of the protein, then bends toward the protein surface assuming an L shape, and ends at Tyr 361 and Ser 365 (Figure 3b). Its shape and dimensions are nearly constant whether a 6-, 12-, or 16-carbon chain is bound. With no side-chain movements beyond what we observe in the HDSC complex, the tunnel can accommodate a fatty acid length of 18 carbons, and with small adjustments of the side chains at the far end of the tunnel even longer fatty acid chains can be accommodated.

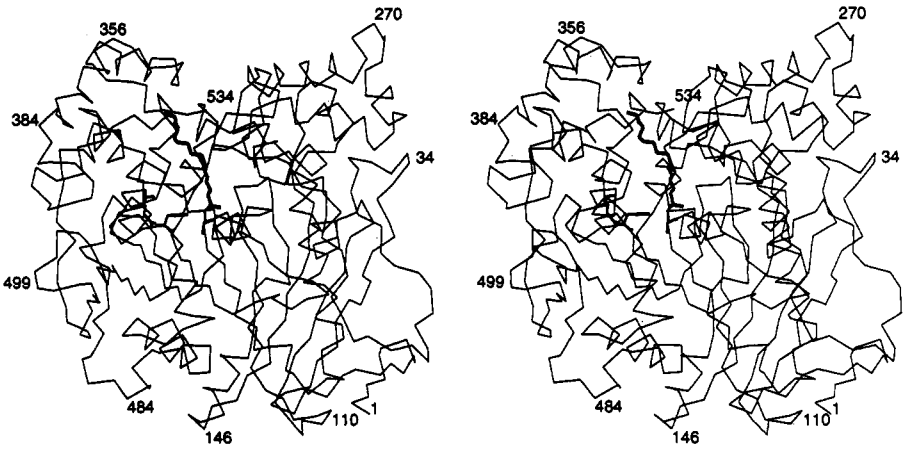

FIGURE 2: Stereo Cα trace of the CRL–HDSC complex. The inhibitor, covalently linked to Ser 209, is shown with a bold line. The catalytic triad residues are shown in full.

Superposition of the complexes with the unliganded open conformation shows that there are no major shifts in the backbone atoms of the protein. The root mean square difference in position for all protein atoms is only 0.36 Å, whereas for the side chains of 25 residues forming the walls of the tunnel the rms deviation is 0.48 Å. This tunnel is also present in the closed conformation of the protein, although it is occluded from the solvent by the flap (Grochulski et al., 1994). The binding tunnel is, thus, performed, and activation requires only conformational changes which expose its mouth. Only small side-chain movements of residues lining the tunnel are required to accommodate the scissile fatty acyl chain. No significant density is observed in the portions of the tunnel left unoccupied by short-chain inhibitors.

The superposition of all the complexes shows that the binding of the common atoms of the alkyl chains is identical, with *trans* conformation along most of the bonds. The hydrocarbon chain conforms to the shape of the tunnel and folds around the side chain of Leu 302. This is achieved by adopting a *gauche*$^-$ conformation at C7–C8 and *gauche*$^+$ conformations at C10–C11 and C11–C12. As a result, C2–C8 and C11–C15 run in nearly perpendicular directions (Figure 3b). A *gauche*$^-$ conformation at C14–C15 directs the last carbon of the alkyl chain in yet another direction.

The mouth of the tunnel is formed by Met 213, Leu 304, Phe 345, and Phe 415. The first six atoms of the hydrocarbon chain run above the helix following the nucleophile elbow (Ollis et al., 1992) and contact the side chains of Met 213, Pro 246, Leu 302, and Leu 304 (Figure 3a,b). Lining the side of the cavity opposite Leu 302 in the region of the bends in the alkyl chain are Pro 246 and Val 534. The chain atoms C12–C17 fill the arm of the tunnel projecting toward the protein surface, making van der Waals contacts with Leu 302, the aliphatic chain of Arg 303, Phe 362, and Phe 366. Ser 365, near the end of the tunnel, is bridged to Ser 300 by a water molecule.

Oxyanion Hole. An oxyanion produced in each of the tetrahedral intermediates is stabilized by interactions in the oxyanion hole, which in CRL was predicted to be formed by the backbone NH atoms of Gly 124 and Ala 210 (Grochulski et al., 1993). The oxyanion analog of each complex makes hydrogen bonds to these residues with distances of 2.7 and 3.0 Å, respectively (Figure 3a,b). These oxygen atoms are positioned near the base of the helix following the nucleophile elbow, indicating that the oxyanion is additionally stabilized by the helix dipole (Hol et al., 1978). Additionally, the amide nitrogen of Gly 123 is oriented toward the oxyanion at a distance ranging from 2.7 Å in the HDSC complexes to 3.0 Å in the MPC complex. Gly 123 apparently is involved in the formation of the oxyanion hole in the HDSC complexes, but the geometry of this potential hydrogen bond is less ideal in the MPC complex, making participation of Gly 123 in oxyanion stabilization ambiguous in this case. Further ambiguity arises from the presence of a water molecule (water 610 in Figure 3a,b) within hydrogen-bonding distance of the amide nitrogen of Gly 123 on the opposite side of the peptide backbone from the oxyanion. The participation of Gly 123, Gly 124, and Ala 210 in formation of the oxyanion hole in the HDSC complexes is similar to the proposed tripartite oxyanion stabilization by Gly 118, Gly 119, and Ala 201 in acetylcholinesterase (Sussman et al., 1991).

O-(1R,2S,5R)-Menthyl Hexylphosphonate Complex. This complex is an analog of the tetrahedral intermediate of the acylation step (I in Figure 1). The positions of the catalytic residues are essentially identical to those in the unliganded lipase. As described above, the hexyl chain inserts into the binding tunnel. The phosphonyl group is covalently bound to Ser 209, and the menthyl moiety, the analog of the alcohol leaving group, binds in a crevice above the catalytic site (Figure 3a). The arrangement around the phosphorus atom of the CRL–MPC complex is that expected for the tetrahedral intermediate (Figure 1), although the geometry is not perfectly tetrahedral. The oxyanion analog settles into the oxyanion hole (see above). The phosphonyl oxygen analog of the leaving alcohol and the covalently modified Oγ atom of Ser 209 are approximately equidistant, ~3.0 Å, from the Nε2 atom of His 449 in an arrangement typical of a bifurcated hydrogen bond. In this arrangement the Nε2 atom of His 449 is the proton donor, whereas in the unliganded enzyme Nε2 is expected to accept a proton from Oγ of Ser 209. The presence of a hydrogen bond from Nδ1 of His 449 to Glu 341 confirms that this histidine is doubly protonated in the complex, as expected from the pH (5.4) of the crystallization. The proposed reaction mechanism also produces a doubly protonated triad histidine in the tetrahedral intermediate.

The menthyl ring of the inhibitor fills a crevice which is occupied by Phe 87 of the flap in the closed conformation of CRL. This ovoid crevice is formed primarily by hydrophobic residues of the oxyanion hole loop, the helix following the catalytic Glu 341, and a Phe 296 from the loop adjacent to the flap. Several hydrophilic residues, His 449, Ser 450, and Glu 208 from the nucleophilic elbow, also form part of this crevice (Figure 3a). The menthyl ring is in a chair conformation with the isopropyl group packing against the phenyl

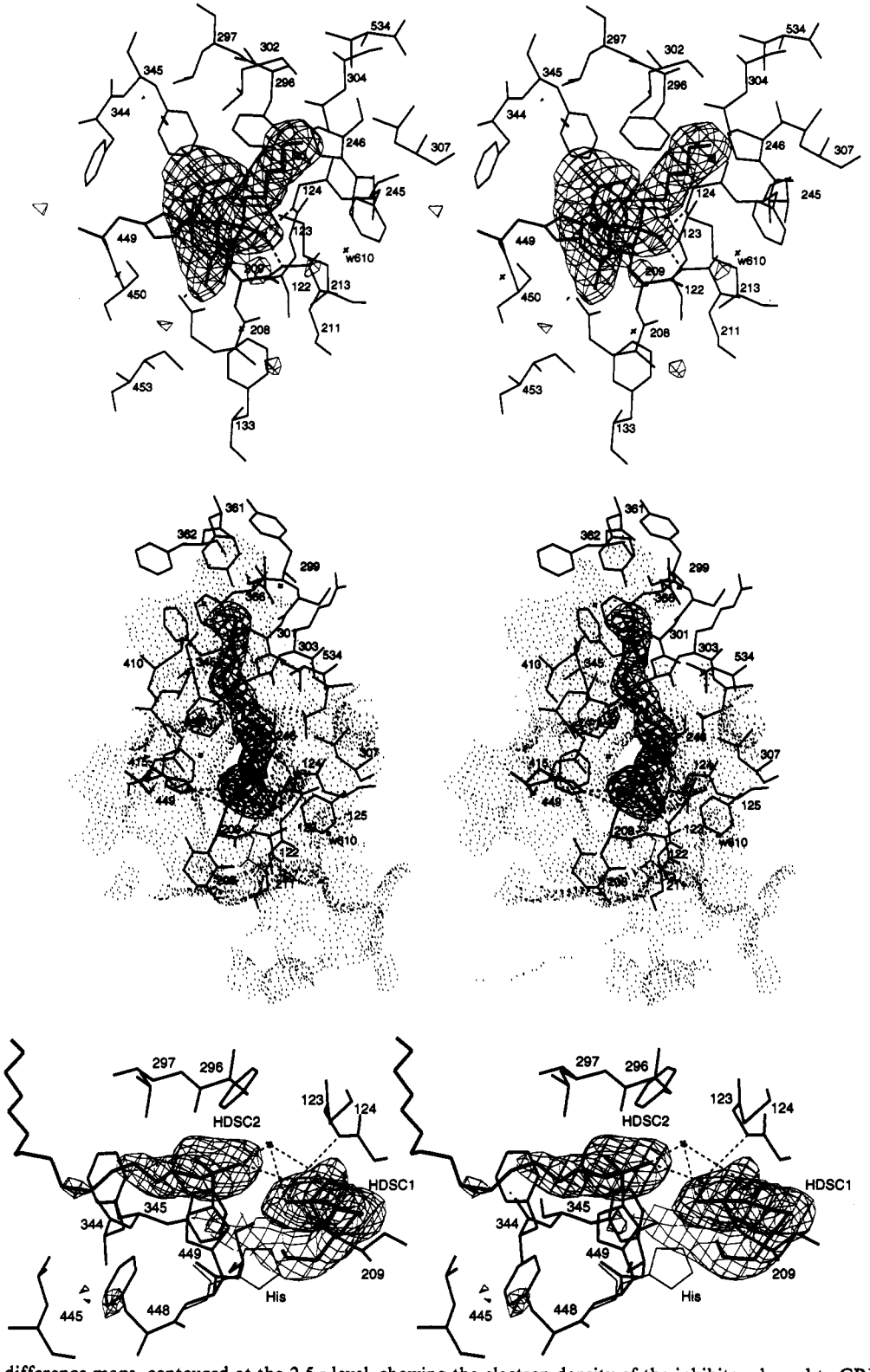

FIGURE 3: Omit difference maps, contoured at the 2.5σ level, showing the electron density of the inhibitors bound to CRL. The inhibitors were excluded from the calculations of F_c. The phosphorus (or sulfur) atom of the inhibitor corresponds to the carboxyl carbon, C1, of a fatty acid chain. The carbon atoms of the inhibitor are, therefore, numbered from 2 to 7 (or 2 to 17 in HDSC) in order to maintain the correspondence to numbering of carbons in a fatty acid chain. Shown are CRL residues within 5-Å distance from an inhibitor. Crosses represent bound solvent molecules. (a, top) $F_o - F_c$ map for the CRL–MPC complex. The inhibitor is modeled in heavy lines. Dashed lines indicate hydrogen bonds to oxygens attached to phosphorus. Ser 209 and His 449 are shown in medium lines. (b, middle) Difference density for the CRL–HDSC complex (HDSC4; inhibitor:enzyme ration of 4:1). The hydrogen bonds of the oxyanion role and His 449 are shown as dashed lines. Dots represent the molecular surface near the entrance to the tunnel as calculated by the program MS (Connelly, 1983) with a probe radius of 1.4 Å. (c, bottom) $F_o - F_c$ map for a CRL–HDSC complex (HDSC120) prepared with an inhibitor:enzyme ratio of 120:1. Shown are residues within 5-Å distance from HDSC2. Note that the His 449 ring has rotated out of its position in the catalytic triad (His, shown in thin lines). Only the first part of the HDSC2 molecule is well ordered.

rings of Phe 296 and Phe 345. The methyl substituent at the other end of the ring abuts Ser 450, primarily interacting with Cβ, and displaces a putative MPD molecule which is bound to Ser 450 in the native open enzyme. The methyl group also

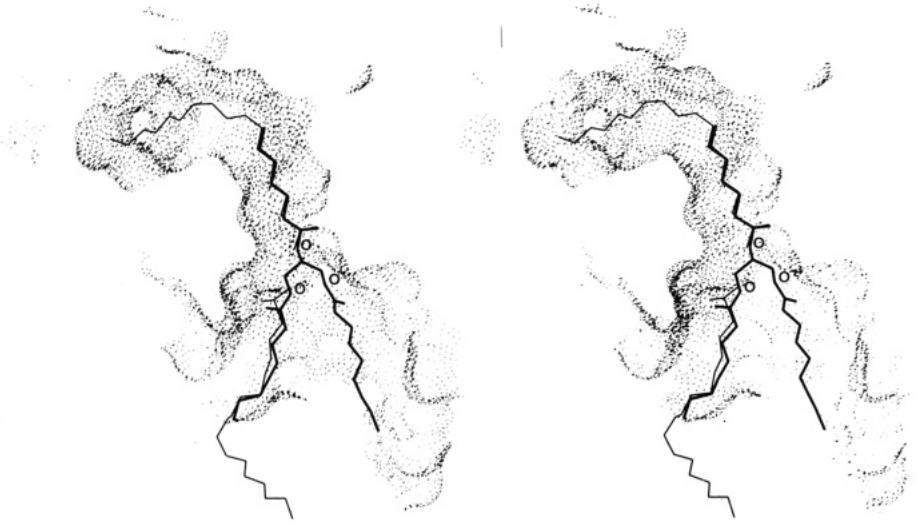

FIGURE 4: Model of tripentanoylglycerol bound to CRL (thick lines) in the tuning fork conformation. The *sn*-2 fatty acyl chain is in the tunnel while the *sn*-1 and *sn*-3 chains are pointing toward the solvent. Glycerol oxygens are marked with the letter O. The positions of chains 1 and 2 of the triacylglycerol are based on the positions of the two bound HDSC molecules (thin lines). Dots represent the molecular surface near the substrate binding site. The wall of the crevice on the right-hand side comes from the flap.

contacts the carbonyl oxygen of Gly 122 and covers a water molecule which bridges Glu 208 and the backbone NH of Gly 122. Since this water molecule is also present in the unliganded and closed structures, these hydrogen bonds probably are important structurally.

Although the protein was incubated with a 1:1 mixture of the S_P and R_P phosphonochloridate diastereomers, only the S_P phosphonate is observed in the crystal structure. Since nucleophilic displacements invert phosphorus centers, this implies that CRL reacted selectively with the S_P diasteromer (priority rules of nomenclature yield an S_P designation for both the starting phosphonyl chloride and the phosphonate complex despite the inversion). To extrapolate this stereochemistry to the hydrolysis of esters, the Ser 209 nucleophile would attack the *re* face of the ester carbonyl.

Sulfonate Complexes. The sulfonate complexes are analogs of the tetrahedral intermediate of the deacylation step (**II** in Figure 1). The alkyl chain binds in the tunnel (Figure 3b), and only its sulfonyl head, with the sulfur atom covalently bound to the Oγ atom of Ser 209, protrudes to the protein surface and is exposed to the solvent. The oxyanion analog makes hydrogen bonds in the oxyanion hole as described previously. The second oxygen atom, the analog of the oxygen derived from the water molecule which attacks the acyl-enzyme complex, and the oxygen atom of Ser 209 are again roughly equidistant from Nϵ2 of His 449, indicating a bifurcated hydrogen bond. The position of this oxygen atom suggests that the water attacks the *si* face of the acyl-enzyme intermediate, the opposite face to that attacked by the serine.

Modeling of Triglyceride Binding. Inhibition of CRL with sulfonyl chloride:enzyme ratios of 10:1 and greater resulted in a second site of covalent modification. In addition to the inhibitor bound to Ser 209, a second inhibitor molecule has covalently modified His 449. These complexes are no longer transition-state analogs, as the modified His side chain is rotated away from its position in the intact triad. The sulfonyl group of the second inhibitor is attached to Nϵ2 of the histidine ring (Figure 3c). The two inhibitor molecules bind in a head to head arrangement and are bridged by two water molecules which hydrogen bond to one oxygen atom from each inhibitor. Only the first five carbons of this second alkyl chain are well ordered. These carbon atoms fold between and make extensive van der Waals contacts with the phenyl rings of Phe 344 and Phe 448. The former becomes well ordered in this complex, in contrast to the unliganded open form of CRL and HDSC complexes at lower ratios. The sulfonyl group of the second inhibitor occupies a space taken by a bound putative MPD molecule in the unliganded open CRL and in complexes with low inhibitor:lipase ratios. The ordering of the Phe 344 side chain by the hydrocarbon chain of the inhibitor suggests that this region is a "sticky" patch which is important in the binding of the substrate. Inhibitor:enzyme ratios as high as 120:1 resulted in no further chemical modifications, despite the accessibility of two other surface His residues, suggesting that the inhibitor molecules are only bound in the hydrophobic area surrounding the active site and that the appearance of the second inhibitor molecule in this region is not coincidental. The rotation of the His 449 side chain away from its position in the triad probably results from the affinity of the inhibitor for this site. Although these complexes cannot be interpreted in terms of the reaction pathway, the alkyl chain of the second inhibitor molecule provides an indication of a likely binding site for a second chain of the natural substrate, triglyceride.

When one fatty acyl chain of a model triglyceride was superimposed on the first molecule of HDSC in the binding tunnel, a neighboring chain could be superimposed on the second HDSC molecule by rotation around C–C bonds. Importantly, the ester bond of this other chain falls in exactly the same position that the sulfonyl group of the second inhibitor molecule does, and a hydrogen bond between the carbonyl oxygen of the ester and Ser 450 is possible. After the positions of the first two fatty acid chains of the triglyceride are fixed, the third fatty acyl chain extends into the solvent and has room to adopt many different conformations. A number of hydrophobic side chains are available for interactions with this hydrocarbon chain. No steric difficulties are encountered in positioning the triglyceride in the binding depression (Figure 4). Similar interactions between the triglyceride and enzyme can be modeled with either the *sn-1,3* or *sn-2* chains in the binding pocket. In either case, the triglyceride molecule is bound in a "tuning fork" conformation.

DISCUSSION

The substrate binding tunnel of CRL is unique among the lipases whose structures have been reported to date and likely

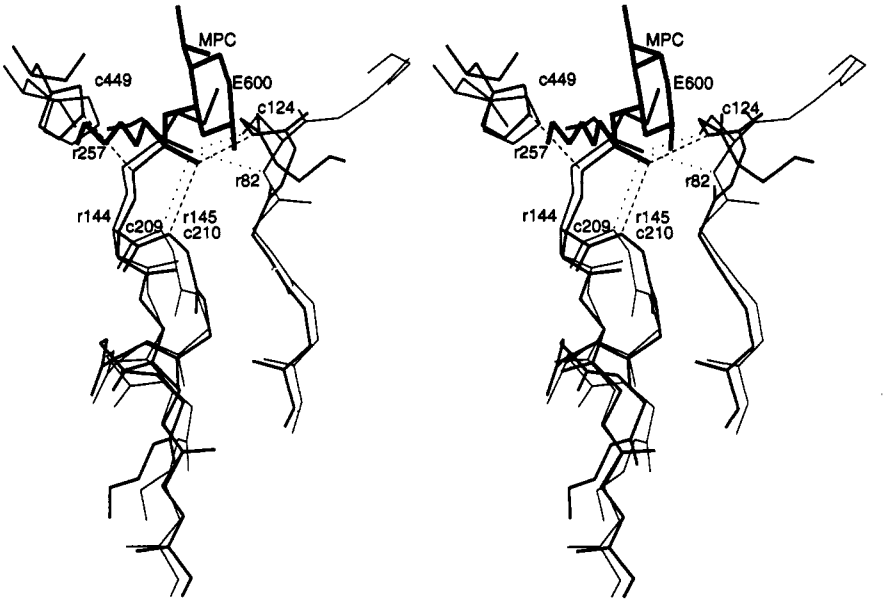

FIGURE 5: Superposition of the RML–E600 (Derewenda et al., 1992) (4tgl, thin lines) and CRL–MPC (thick lines) complexes. Cα atoms of five residues one each side of the catalytic serine in both molecules were used to calculate the transformation matrix. Letters c and r precede the residue numbers of CRL and RML, respectively. The stereochemistry of the phosphorus is identical in both complexes. Hydrogen bonds are shown as dashed lines for CRL and as dotted lines for RML.

explains why CRL is more stereoselective than other lipases toward substrates that have a stereocenter in the acid portion. Nevertheless, the inhibitor binding by CRL shows some similarity to the inhibitor binding by RML. The structures of the RML–inhibitor complexes (Brzozowski et al., 1992; Derewenda et al., 1992) (PDB codes 4tgl and 5tgl) were superimposed on the CRL complexes using the strand–turn–helix motif around the catalytic Ser as an anchor. After superposition, the alkyl chain of the inhibitor in the RML complex (4tgl) and the hexyl chain of the CRL–MPC complex overlap almost perfectly (Figure 5). The oxyanion analogs and one of the NH groups forming the oxyanion holes in RML and CRL are also in nearly identical positions (Figure 5). The second NH of the oxyanion hole comes from slightly different directions in these two lipases. The conformation of the loop contributing to the oxyanion hole in CRL is very similar to that of the corresponding loop in acetylcholinesterase (AChE) (Sussman et al., 1991). Examination of the published diagrams of the HPL–phospholipid and cutinase–diethyl *p*-nitrophenyl phosphate (E600) complexes (van Tilbeurgh et al., 1993) indicates that the position of the scissile bond and the orientation of the oxyanion hole relative to the catalytic Ser are very similar in all of these enzymes, suggesting that the reaction mechanisms are identical. We have previously postulated that CRL and the *Geotrichum candidum* lipase (GCL) function similarly (Grochulski et al., 1993). On the basis of these comparisons, we propose that all lipases which share the essential features of the α,β-hydrolase fold (Ollis et al., 1992) orient the hydrolyzed ester of the substrate and the first few carbons of the fatty acyl chain in an identical manner.

The stereochemistry at the phosphorus center in the CRL–MPC complex and in the RML complex is identical. In both cases the S_P phosphonate is observed, indicating that the nucleophilic attack of the ester occurs from the *re* face in both enzymes. Given the similarity of the enzyme folds and position of the oxyanion holes, this is probably common to AChE, GCL, HPL, and cutinase as well.

In RML and cutinase, the fatty acyl chain lies in a groove on the surface of the protein. In contrast, the CRL binding site is not a groove but is covered by other surface loops to form a tunnel into which the alkyl chain binds. How the fatty acyl chain enters the tunnel is not yet clear. One possbility is that it simply inserts into the existing tunnel. The flexibility of the alkyl chain and the fact that the tunnel is not straight suggest that this process might be difficult and slow, like pushing a string into a hole. A second possibility is a concerted movement of subdomains of the protein to open the tunnel into a groove which then closes around the bound fatty acyl chain. Comparison of the structures of AChE and GLC showed that these enzymes can be divided into two subdomains of roughly equivalent size (Cygler et al., 1993). CRL can be similarly divided into subdomains, and the catalytic site and binding tunnel reside at the interface between the subdomains. These subdomains could conceivably "breathe" to allow access to the binding site from a sideways approach, rather than end on. Fatty acyl binding in this manner would be comparable to that of RML. However, this scenario requires substantial movement of the subdomains and possibly also structural rearrangements of some loops. As yet, there is no evidence which suggests that any movements of that nature occur.

The removal of the fatty acid chain produced by hydrolysis also warrants attention. The bound hydrocarbon chain makes many hydrophobic contacts with the residues lining the tunnel. One might expect that a significant driving force would be required to remove the fatty acid from this favorable environment. Glu 208 and Asp 452, near the mouth of the tunnel, may be instrumental in this regard. Electrostatic potential calculations show that this region has one of the most negative potentials in the entire protein (Figure 6). This negative potential may provide an electrostatic driving force facilitating the release of the negatively charged fatty acid produced by hydrolysis. The binding of cholesterol esterase, a homologue of CRL (Cygler et al., 1993), to diglyceride monolayers is independent of pH, whereas binding to fatty acid monolayers is strongly pH dependent and inversely related to the amount of negative charge of the lipid (Tsujita & Brockman, 1987). Since CRL is homologous to cholesterol esterase, similar behavior is likely and would be consistent with an electrostatic influence on product release. Interest-

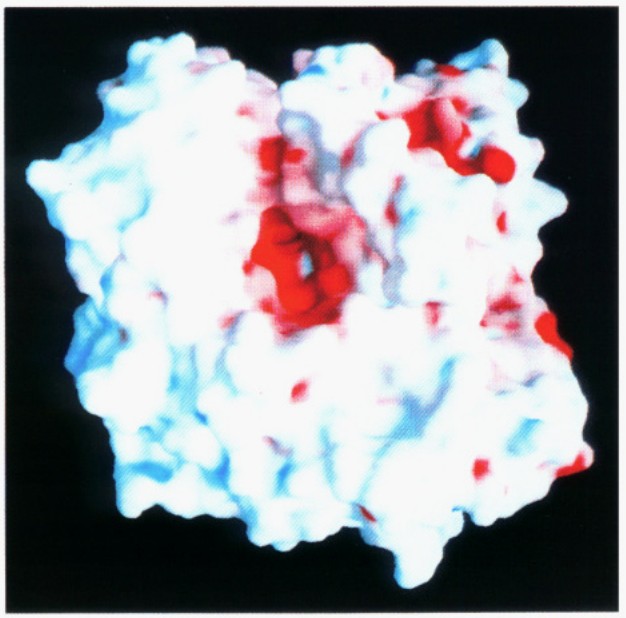

FIGURE 6: View of the molecular surface of CRL. The colors correspond to electrostatic potential with red as negative and blue as positive. The hydrogens of the polypeptide main chain were included in the calculations. The entrance to the tunnel is apparent in the center of the protein. The blue area on the right-hand side of the tunnel corresponds to the position of the oxyanion hole. This figure was produced with the program GRASP (Nicholls et al., 1992).

ingly, phosphorylation of a tyrosine residue in the binding site of adipocyte lipid-binding protein abolishes fatty acid binding and changes the electrostatic potential of the binding cavity from positive to negative (Cowan et al., 1993). Thus, electrostatic mechanisms of product release are implicated in both CRL and adipocyte lipid-binding protein.

The binding tunnel of CRL also differs from the ligand binding pockets of the fatty acid and retinol binding proteins (Cowan et al., 1990, 1993; Benning et al., 1992; Xu et al., 1993; Sacchettini et al., 1989). Predictably, the residues interacting with the ligand are primarily hydrophobic in both CRL and the fatty acid binding proteins. However, the orientations of the fatty acid chains in the respective binding cavities are opposite. In the fatty acid binding proteins, the carboxyl group of the bound fatty acid interacts with hydrophilic groups at the closed end of the pocket, with the hydrocarbon tail directed toward the solvent. In CRL, the hydrocarbon chain enters the tunnel, leaving the hydrophilic head group exposed to the solvent. Additionally, the binding pockets of the fatty acid binding proteins are large enough to accommodate water molecules and ions in addition to the ligand. The binding pocket in CRL is only large enough to accommodate the fatty acid chain, and no density which could be interpreted as ordered water molecules or ions is observed in the channel, even in the unliganded state.

ACKNOWLEDGMENT

We gratefully acknowledge the technical assisstance of Yunge Li and Marc Desrochers.

REFERENCES

Benning, M. M., Smith, A. F., Wells, M. A., & Holden, H. M. (1992) *J. Mol. Biol. 228*, 208.
Boland, W., Frršl, C., & Lorenz, M. (1991) *Synthesis 12*, 1049.
Brady, L., Brzozowski, A. M., Derewenda, Z. S., Dodson, E., Dodson, G. G., Tolley, S., Turkenburg, J. P., Christiansen, L., Hugh-Jensen, B., Norskov, L., Thim, L., & Menge, U. (1990) *Nature 343*, 767.
Brünger, A. T. (1992) *X-PLOR (Version 3.1): A system for X-ray crystallography and NMR*, Yale University Press, New Haven, CT.
Brzozowski, A. M., Derewenda, U., Derewenda, Z. S., Dodson, G. G., Lawson, D. M., Turkenburg, J. P., Bjorkling, F., Huge-Jensen, B., Patkar, S. A., & Thim, L. (1991) *Nature 351*, 491.
Chapus, C., & Sémériva, M. (1976) *Biochemistry 15*, 4988.
Chapus, C., Sémériva, M., Bovier-Lapierre, C., & Desnuelle, P. (1976) *Biochemistry 15*, 4980.
Connolly, M. L. (1983) *J. Appl. Crystallogr. 16*, 548.
Cowan, S. W., Newcomer, M. E., & Jones, T. A. (1990) *Proteins: Struct., Funct., Genet. 8*, 44.
Cowan, S. W., Newcomer, M. E., & Jones, T. A. (1993) *J. Mol. Biol 230*, 1224.
Cygler, M., Schrag, J. D., Sussman, J. L., Harel, M., Silman, I., Gentry, M. K., & Doctor, B. P. (1993) *Protein Sci. 2*, 366.
Derewenda, U., Brzozowski, A. M., Lawson, D. L., & Derewenda, Z. S. (1992) *Biochemistry 31*, 1532.
Grochulski, P., Li, Y., Schrag, J. D., Bouthillier, F., Smith, P., Harrison, D., Rubin, B., & Cygler, M. (1993) *J. Biol. Chem. 268*, 12843.
Grochulski, P., Li, Y., Schrag, J. D., & Cygler, M. (1994) *Protein Sci. 3*, 82.
Hol, W. G. J., van Duijnen, P. T., & Berendsen, H. J. C. (1978) *Nature 273*, 443.
Jones, T. A. (1978) *J. Appl. Crystallogr. 11*, 268.
Martinez, C., DeGues, P., Lauwereys, M., Matthyssens, G., & Cambillau, C. (1992) *Nature 356*, 615.
Nicholls, A., Sharp, K. A., & Honig, B. (1991) *Proteins: Struct., Funct., Genet. 11*, 282.
Ollis, D. L., Cheah, E., Cygler, M., Dijkstra, B., Frolow, F., Franken, S. M., Harel, M., Remington, S. J., Silman, I., Schrag, J. D., Sussman, J. L., Verscheuren, K. H. G., & Goldman, A. (1992) *Protein Eng. 5*, 197.
Sacchettini, J. C., Gordon, J. I., & Banaszak, L. J. (1989) *J. Mol. Biol. 208*, 327.
Schrag, J. D., Li, Y., Wu, S., & Cygler, M. (1991) *Nature 351*, 761.
Sussman, J. L., Harel, M., Frolow, F., Oefner, C., Goldman, A., Toker, L., & Silman, I. (1991) *Science 253*, 872.
Tsujita, T., & Brockman, H. L. (1987) *Biochemistry 26*, 8423.
van Tilbeurgh, H., Egloff, M.-P., Martinez, C., Rugani, N., Verger, R., & Cambillau, C. (1993) *Nature 362*, 814.
Winkler, F. K., D'Arcy, A., & Hunziker, W. (1990) *Nature 343*, 771.
Xu, Z., Bernlohr, D. A., & Banaszak, L. J. (1993) *J. Biol. Chem. 268*, 7874.
Zhao, K., & Landry, D. W. (1993) *Tetrahedron 48*, 363.